

Heat Transfer in Adhesively Bonded Honeycomb Core Panels

K. Daryabeigi*

NASA Langley Research Center, Hampton, Virginia 23681

The influence of adhesive thickness and thermal properties on the overall heat transfer through an adhesively bonded honeycomb core panel over the temperature range of 250–500 K was investigated. The combined radiation and conduction heat transfer was modeled using a finite volume numerical formulation. The numerical model was validated by comparison with published experimental effective thermal conductivity measurements. It was found that the adhesive layer could cause significant augmentation of heat transfer through the honeycomb panel. A parametric study was conducted to investigate the influence of adhesive thickness, thermal conductivity, and emissivity on the overall heat transfer through the panel.

Nomenclature

A	= cross-sectional area
b	= side length of honeycomb hexagonal cell
F	= radiation shape factor
k	= thermal conductivity
L	= panel height (core plus facesheets)
L'	= honeycomb core height
q''	= heat flux
r	= radial coordinate
T	= temperature
t	= thickness
z	= axial coordinate
β	= dimensionless adhesive thickness
δ	= Kronecker delta
ε	= emissivity
κ	= dimensionless adhesive thermal conductivity
λ	= height to diameter ratio for honeycomb cell
ξ	= dimensionless effective thermal conductivity
σ	= Stefan–Boltzmann radiation constant

Subscripts

ad	= adhesive
e	= effective
f	= foil
g	= gas
r	= radiant

Introduction

THE Swann and Pittman¹ semi-empirical relationship has been used throughout the aerospace industry as the standard model for determining combined radiation and gas and solid conduction heat transfer in honeycomb core panels. Published results² of measured effective thermal conductivity of an adhesively bonded honeycomb core panel in the temperature range of 300–500 K using a radiant step heating technique³ yielded results that were significantly different from the Swann and Pittman predictions.¹ The variation of the measured thermal conductivity with average panel temperature

and the Swann and Pittman predictions¹ are shown in Fig. 1. Error bars represent $\pm 5\%$ uncertainty for experimental measurements. The difference between predictions and measurements increased with increasing temperature, and the root mean square deviation between the measurements and Swann and Pittman predictions¹ was 18.2%. The discrepancy was believed to be caused by the adhesive layer because the Swann and Pittman prediction does not include an adhesive layer in the model. Note that the effective thermal conductivity measurement of a honeycomb core panel is a nontrivial experiment and that the results are not always independent of the technique used. The measured effective thermal conductivities of the panel using the standard steady-state techniques of guarded hot plate⁴ and heat flow meter⁵ were significantly higher than the reported radiant step heating data and were determined to be inaccurate.⁶

The purpose of the present investigation was to determine the influence of the adhesive layer on the overall heat transfer through the honeycomb core panel. This was accomplished by a finite volume numerical solution to the governing combined radiation/conduction heat transfer problem. The results were then compared with the Swann and Pittman predictions¹ and the experimental results of Ref. 2. Finally, a parametric study was conducted to investigate the influence of adhesive thickness, thermal conductivity, and emissivity on the overall heat transfer.

Background

Various researchers have investigated heat transfer in honeycomb core structures. Most of the experimental work reported in the literature has been limited to panels with the honeycomb core brazed or spot welded to the facesheets. None of the available experimental or analytical literature has considered adhesively bonded honeycomb structures. Swann and Pittman¹ used a finite difference numerical model to study combined conduction and radiation in honeycomb structures and used their results to derive a semi-empirical relationship for the effective thermal conductivity as a function of geometric parameters and material properties. Stroud⁷ measured effective thermal conductivities of four brazed honeycomb core panels over a temperature range of 670–1050 K and showed a root mean square deviation of 7% between his measured values and predictions using the Swann and Pittman semi-empirical relationship.¹ Fairbanks⁸ analytically investigated the effective thermal conductivity of evacuated square cell honeycomb cores for heat flow lateral to the principal axes of the cells. Jones⁹ performed an analytical study of combined solid conduction and radiation heat transfer through evacuated honeycomb core panels. He investigated the influence of core cell aspect ratio, internal surface emissivity, and the thermal resistance in the joint between the core material and facesheets. Copenhaver et al.¹⁰ used the finite element numerical technique to model combined conduction/radiation in honeycomb core panels and used parameter estimation techniques in conjunction with experimental heating data to estimate specific heat of the facesheets, emissivity in the core, and the conduction area of the core.

Presented as paper 2001-2825 at the AIAA 35th Thermophysics Conference, Anaheim, CA, 11–14 June 2001; received 23 July 2001; revision received 10 January 2002; accepted for publication 29 January 2002. Copyright © 2002 by the American Institute of Aeronautics and Astronautics, Inc. No copyright is asserted in the United States under Title 17, U.S. Code. The U.S. Government has a royalty-free license to exercise all rights under the copyright claimed herein for Governmental purposes. All other rights are reserved by the copyright owner. Copies of this paper may be made for personal or internal use, on condition that the copier pay the \$10.00 per-copy fee to the Copyright Clearance Center, Inc., 222 Rosewood Drive, Danvers, MA 01923; include the code 0887-8722/02 \$10.00 in correspondence with the CCC.

*Aerospace Engineer, Metals and Thermal Structures Branch, Senior Member AIAA.

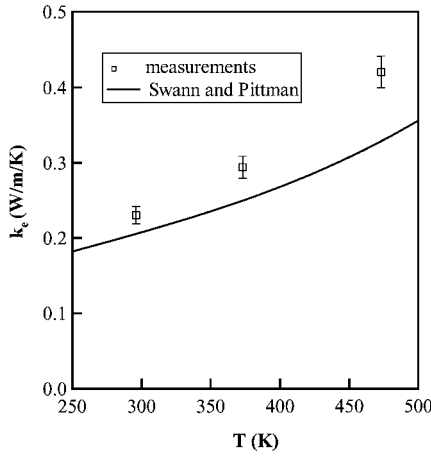


Fig. 1 Comparison of the measured effective thermal conductivity² with Swann and Pittman model.¹

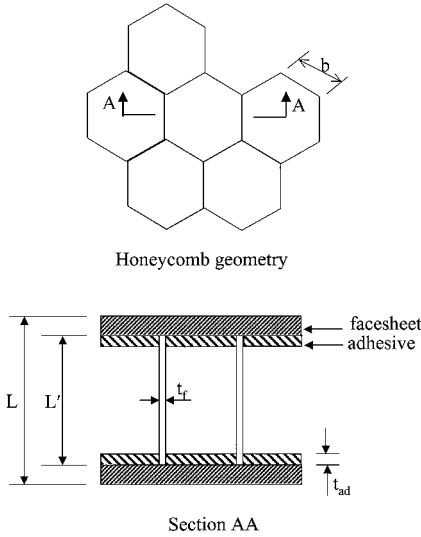


Fig. 2 Schematic of the honeycomb core panel (not to scale).

Edwards et al.¹¹ experimentally studied natural convection in honeycomb structures and determined the critical Rayleigh number for the onset of natural convection. For the honeycomb core panel studied here, the critical Rayleigh number for the onset of natural convection and the maximum Rayleigh number were determined to be 61,000 (Ref. 11) and 7900, respectively. Therefore, natural convection was not considered as a mode of heat transfer in the present study.

Honeycomb Core Panel Description

The honeycomb core panel used in this study was made of titanium 3Al-2.5V with a density of 94.5 kg/m³. A schematic of the honeycomb core panel is shown in Fig. 2. The core height was 25.4 mm and consisted of hexagonal cells with 4.76-mm side length and 0.035-mm foil thickness. The facesheets were 1.6-mm-thick titanium 6-22-22. The honeycomb core was attached to the facesheets using a polyimide adhesive film on a woven glass carrier. The adhesive thickness on each facesheet was determined to be 0.94 mm.

Published results were used for the thermal conductivity of the titanium honeycomb core,¹² titanium facesheets,¹³ and air.¹⁴ The thermal conductivity of the adhesive layer was unknown, but was expected to be dominated by the thermal conductivity of woven glass (estimated to be in the range of 0.3–0.5 W/m/K at room temperature).¹⁵ For the present study, it was assumed that the thermal conductivity of the adhesive was either 10 or 50 times the thermal conductivity of air over the temperature range of interest. The resulting adhesive thermal conductivity at room temperature was in

the range of 0.25–1.25 W/m/K, which covered the range of thermal conductivities for woven glass and typical adhesives. The dimensionless adhesive thermal conductivity κ was defined as the ratio of the thermal conductivity of adhesive to air:

$$\kappa = k_{ad}/k_g \quad (1)$$

The emissivities of titanium foil and adhesive layer were assumed to be independent of temperature in the temperature range of interest and equal to 0.3 (Ref. 16) and 0.8 (Ref. 17), respectively.

Swann and Pittman Model¹

Swann and Pittman developed a semi-empirical model for heat transfer through brazed and spot welded honeycomb core panels.¹ They neglected the thermal contribution of the facesheets, developed an empirical relationship for modeling radiation in the honeycomb core enclosure, and used a parallel thermal network model for modeling solid and gas conduction through the honeycomb core. The effective thermal conductivity k_e is given by¹

$$k_e = k_f(\Delta A/A) + k_g[1 - (\Delta A/A)] + k_r \quad (2)$$

where $\Delta A/A$ is the ratio of the cross-sectional areas of the solid core to the overall honeycomb cell. The radiant effective conductivity k_r is given by¹

$$k_r = 0.664(\lambda + 0.3)^{-0.69} \varepsilon^{1.63(\lambda + 1)^{-0.89}} L' \sigma (T_1 + T_2)(T_1^2 + T_2^2) \quad (3)$$

where T_1 and T_2 are the temperatures of the facesheets. It is assumed that the facesheets and honeycomb core have the same emissivity.¹ The radiant effective conductivity is an empirical relationship developed by Swann and Pittman by comparison with results of a finite difference numerical model of the combined conduction/radiation heat transfer in the honeycomb cell.¹

Combined Conduction/Radiation Heat Transfer in Honeycomb Panel

A steady-state finite volume numerical method was used to solve the combined conduction/radiation heat transfer in the adhesively bonded honeycomb core panel. The governing equations were applied to a volume representing one cell of the honeycomb core and the associated facesheets and adhesive layers. The hexagonal core of the honeycomb was approximated as having a circular cross section, with its equivalent diameter obtained by equating the perimeters of the hexagonal and circular cross sections.¹ This approximation reduced the problem to an axisymmetric case. A schematic of the simulated axisymmetric geometry is shown in Fig. 3. The governing partial differential equation for conduction heat transfer is

$$\frac{1}{r} \frac{\partial}{\partial r} \left(r k \frac{\partial T}{\partial r} \right) + \frac{\partial}{\partial z} \left(k \frac{\partial T}{\partial z} \right) = 0 \quad (4)$$

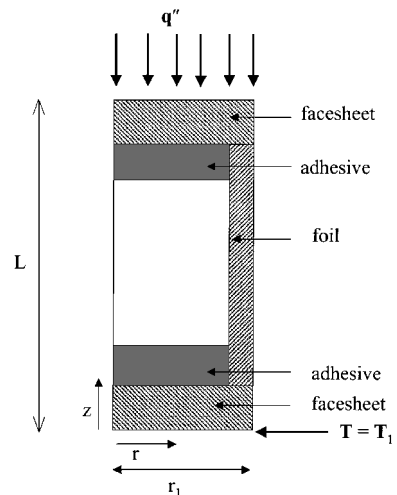


Fig. 3 Schematic of axisymmetric geometry for the numerical model (not to scale).

The boundary conditions are

$$k \frac{\partial T}{\partial z}(L, r) = q'' \quad (5a)$$

$$T(0, r) = T_1 \quad (5b)$$

$$|T(z, 0)| < \infty \quad (5c)$$

$$\frac{\partial T}{\partial r}(z, r_1) = 0 \quad (5d)$$

The first two boundary conditions represent an applied constant heat flux and a constant temperature condition applied to the two facesheets of the honeycomb core panel, respectively. The third boundary condition implies finite temperature at $r = 0$, whereas the last boundary condition represents an adiabatic condition due to temperature symmetry at the cell boundary. The finite volume formulation of the conservation of energy equation with temperature-dependent thermal properties was utilized.¹⁸

The radiant heat fluxes were included in the energy balance for those control volume cells involved in the radiation exchange in the honeycomb enclosure. The radiant heat fluxes were calculated at each iteration by performing radiation exchange analysis in the enclosure assuming gray surfaces, with each control volume cell assumed to be isothermal with uniform surface radiosity, and, furthermore, under the assumption that both emitted and reflected radiation were diffuse. The incident radiant heat flux at each control volume surface in the honeycomb enclosure involved in radiation exchange was calculated from¹⁹

$$q''_{r,i} = \sum_{k=1}^N \Lambda_{ik} \sigma T_k^4, \quad 1 \leq i \leq N \quad (6)$$

where

$$\Lambda_{ik} = \varepsilon_i / (1 - \varepsilon_i) (\delta_{ik} - \Psi_{ik}) \quad (7a)$$

$$\Psi_{ik} = \Phi_{ik}^{-1} \quad (7b)$$

$$\Phi_{ik} = [\delta_{ik} - (1 - \varepsilon_i) F_{A_i-A_k}] / \varepsilon_i \quad (7c)$$

where N was the total number of control volume surfaces involved in radiation exchange in the enclosure, ε_i was the surface emissivity for each control volume cell, and $F_{A_i-A_k}$ was the shape factor for radiation exchange between surfaces designated as A_i and A_k . The shape factors for the radiation exchange were calculated using the shape factor equations provided by Swann and Pittman¹ for the same geometry.

The nonlinear set of equations resulting from the numerical finite volume form of the governing equations and boundary conditions [Eqs. (4) and (5)], with the radiant flux defined in Eq. (6), was solved using the modified Newton–Raphson method (see Ref. 20). Once the numerical solution had converged, the effective thermal conductivity k_e was calculated based on the applied heat flux, the converged temperature difference between the two facesheets ΔT , and the overall panel height using the Fourier's law of heat conduction¹⁴:

$$k_e = q'' L / \Delta T \quad (8)$$

Results and Discussion

The finite volume numerical model was applied to the honeycomb core panel geometry without any adhesive layer to assess the accuracy of the numerical results by comparison with the Swann and Pittman predictions.¹ The finite volume numerical results and the Swann and Pittman predictions are shown in Fig. 4, where the effective thermal conductivities are plotted vs average honeycomb panel temperature, defined as the arithmetic mean of the two facesheet temperatures. The difference between the Swann and Pittman model and the finite volume numerical predictions had a root mean square

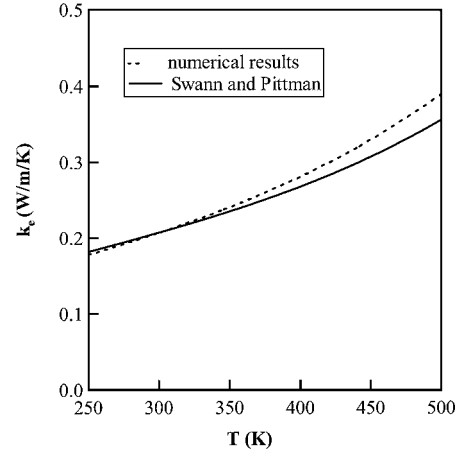


Fig. 4 Comparison of numerical predictions and Swann and Pittman model¹ for honeycomb core panel without adhesive.

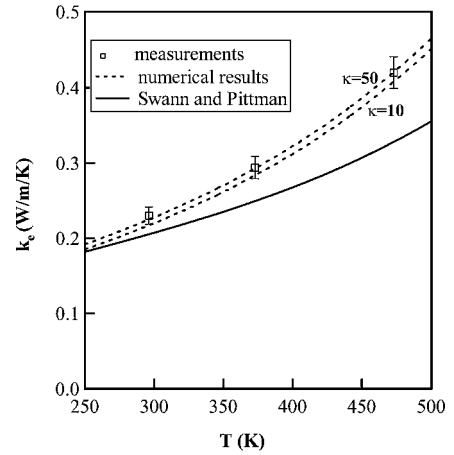


Fig. 5 Comparison of numerical predictions and measurements² for adhesively bonded honeycomb core panel.

deviation of 4.9%, thus validating the numerical model for predicting heat transfer in honeycomb core panels without adhesive bonding.

The numerical results for the adhesively bonded honeycomb core panel for dimensionless adhesive thermal conductivity of 10 and 50 are shown in Fig. 5. The published experimental data² and the Swann and Pittman predictions¹ are also shown. The numerical results matched the experimental measurements within the experimental uncertainty range. The difference between the numerical predictions and experimental data had root mean square deviations of 4.2 and 1.3% for κ of 10 and 50, respectively. The close agreement between numerical and experimental results² validated the numerical model for adhesively bonded honeycomb core panels. Furthermore, they clearly demonstrate that the adhesive layer has a significant effect on the overall thermal performance of honeycomb core panels and should not be ignored in the calculations.

The finite volume numerical model was used to study parametrically the effects of adhesive thickness and thermal conductivity on the effective thermal conductivity. The following dimensionless parameters were used:

$$\beta = t_{ad} / L' \quad (9)$$

$$\xi = \frac{k_e(\beta, \varepsilon, \kappa)}{k_e(\beta = 0, \varepsilon = 0.3)} \quad (10)$$

where β , the dimensionless adhesive thickness, is the ratio of adhesive thickness to honeycomb core height. The dimensionless effective thermal conductivity ξ was defined as the ratio of the effective

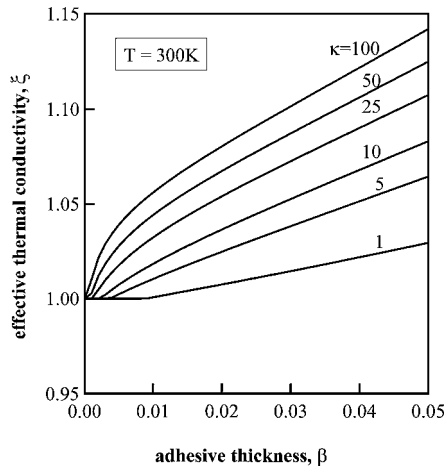


Fig. 6a Variation of effective thermal conductivity with adhesive thickness, 300 K.

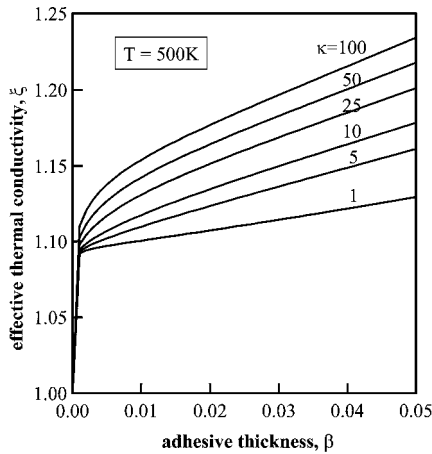


Fig. 6b Variation of effective thermal conductivity with adhesive thickness, 500 K.

thermal conductivities of the adhesively bonded panel to the panel without adhesive. Here, β was varied between 0 and 0.05, with 0 representing a construction with no adhesive. The geometry studied experimentally in this investigation had $\beta = 0.037$. For radiation exchange calculations in the honeycomb enclosure, it was assumed that the emissivity of the lower and upper surfaces of the enclosure were either equal to the emissivity of the facesheets ($\varepsilon = 0.3$) for $\beta = 0$, or equal to the emissivity of the adhesive ($\varepsilon = 0.8$) for $\beta > 0$. Data were obtained for dimensionless adhesive thermal conductivity of 1, 5, 10, 25, 50, and 100. All of the other parameters were kept fixed at the values corresponding to the geometry studied in this investigation.

The results for average panel temperatures of 300 and 500 K are presented in Figs. 6a and 6b, respectively. Data are presented as dimensionless effective thermal conductivity ξ vs β for various values of κ . Results illustrate variation of effective thermal conductivity augmentation with adhesive thickness and adhesive thermal conductivity. All of the data converged to unity when the adhesive thickness was zero. The effective thermal conductivity increased with increasing adhesive thickness and increasing adhesive thermal conductivity. The data for $\kappa = 1$ illustrated the influence of adhesive emissivity and thickness on the radiation heat transfer. Here, the adhesive did not change the conduction heat transfer through the geometry because it had the same thermal conductivity as air, and, thus, the effect of the adhesive on the radiation heat transfer could be isolated. The adhesive had a higher emissivity than the facesheets, and the adhesive thickness changed the overall height of the enclosure for radiation exchange. For the data at 300 K and $\kappa = 1$, ξ

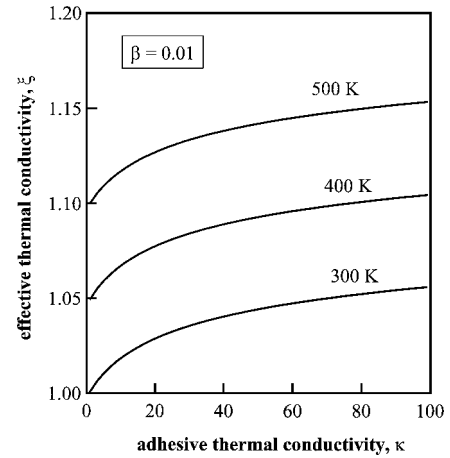


Fig. 7 Variation of effective thermal conductivity with adhesive thermal conductivity.

maintained a value near unity for β between 0 and 0.01 and then gradually increased at a constant slope with increasing β . The data for $\kappa > 1$ exhibited a larger increase in the effective thermal conductivity with increasing adhesive thickness, with ξ also increasing with increasing adhesive thermal conductivity. The higher increases for $\kappa > 1$ compared to $\kappa = 1$ were due to higher solid conduction heat transfer because of the adhesive. In the absence of the adhesive layers, heat is conducted from the facesheet to the foil through the small cross-sectional area of the foil, $6bt_f$ (Fig. 2). In the presence of the adhesive layer, heat is also transferred from the facesheet to the adhesive layer and then from the adhesive layer to the foil through an area equal to $6bt_{ad}$. Depending on the thermal conductivity and thickness of the adhesive layer, this added path for conduction of heat from the facesheet to the foil through the adhesive could result in higher heat conduction rates through the overall honeycomb core panel. For the data at 500 K, ξ increased rapidly from 1 to approximately 1.1 in the presence of an infinitesimal adhesive thickness, irrespective of the adhesive thermal conductivity. This sudden increase compared to data at 300 K is due to higher radiation heat transfer at this higher temperature caused by the higher emissivity of the adhesive compared to the facesheet. Again, ξ increased with increasing κ due to higher solid conduction from the facesheets to the foil through the adhesive layers.

The variation of effective thermal conductivity with adhesive thermal conductivity for $\beta = 0.01$ and for average panel temperatures of 300, 400, and 500 K is shown in Fig. 7. The effective thermal conductivity increases with increasing temperature. Furthermore, the effective thermal conductivity increases rapidly with increasing κ for $1 \leq \kappa \leq 30$ and then increases at a lower rate for $\kappa > 30$. At $\kappa = 100$, the adhesive thermal conductivity approaches the thermal conductivity of the titanium facesheets, and the problem reduces to heat transfer in a honeycomb structure with an effectively thicker facesheet and smaller foil height.

All of the reported results so far have used an adhesive emissivity of 0.8. The variation of dimensionless effective thermal conductivity with adhesive emissivity for $\beta = 0.01$, $\kappa = 1$, and for average panel temperatures of 300 and 500 K is shown in Fig. 8. Adhesive emissivity was varied between 0.1 and 0.9. Because the adhesive has the same thermal conductivity as air ($\kappa = 1$), the results illustrate the influence of adhesive emissivity. The data at 500 K are more sensitive to adhesive emissivity compared to the data at 300 K, due to higher radiation heat transfer at the higher temperature. The data at 300 and 500 K exhibit a higher effective thermal conductivity compared to the honeycomb core panel without adhesive ($\varepsilon = 0.3$) at adhesive emissivities larger than 0.8 and 0.6, respectively. With reference to Eq. (3), the presence of the adhesive has resulted in a lower effective height of the honeycomb core for radiation interchange L' , therefore, adhesive emissivities higher than that of the bare facesheets are required to increase the contribution of the radiation heat transfer component of the effective thermal conductivity.

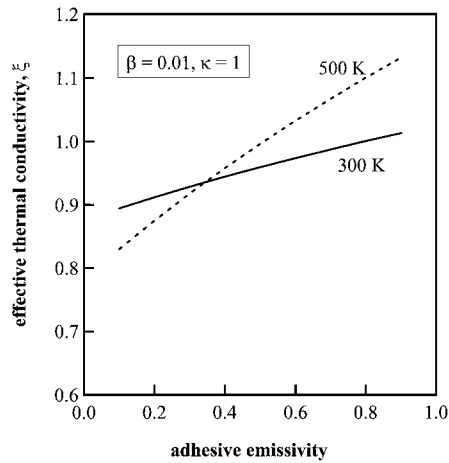


Fig. 8 Variation of effective thermal conductivity with adhesive emissivity.

Conclusions

The combined conduction and radiation heat transfer in an adhesively bonded honeycomb core panel was modeled using a finite volume numerical formulation. It was found that the adhesive layer augmented heat transfer through the honeycomb core panel. The augmentation increased with increasing adhesive thickness, thermal conductivity, emissivity, and average specimen temperature. The adhesive layer provided a larger surface area with higher thermal conductivity to conduct heat from the facesheets to the foils than did the foil edge. The higher emittance of the adhesive also resulted in higher radiation heat transfer. This augmentation of heat transfer due to radiation increased with increasing specimen temperature. These results suggest that ignoring the adhesive in the heat transfer through adhesively bonded honeycomb core panels could lead to significant errors.

References

- ¹Swann, R. T., and Pittman, C. M., "Analysis of Effective Thermal Conductivities of Honeycomb-Core and Corrugated-Core Sandwich Panels," NASA TN D-714, April 1961.
- ²Taylor, R. E., Taylor, D. L., Gembarovic, J., and Ferrier, J., "Investigation of the Thermal Properties of a Honeycomb Material," Thermophysical Properties Research Lab., Rept. TPRL 2259, West Lafayette, IN, Aug. 1999.
- ³American Society for Testing and Materials Standard E 1461, "Standard Test Method for Thermal Diffusivity of Solids by the Flash Method," *Annual*

Book of ASTM Standards, Vol. 14.02, American Society for Testing and Materials, West Conshohocken, PA, 2000, pp. 575–582.

⁴American Society for Testing and Materials Standard C 177, "Standard Test Method for Steady-State Heat Flux Measurements and Thermal Transmission Properties by Means of the Guarded-Hot-Plate Apparatus," *Annual Book of ASTM Standards*, Vol. 4.06, American Society for Testing and Materials, West Conshohocken, PA, 2000, pp. 20–41.

⁵American Society for Testing and Materials Standard C 518, "Standard Test Method for Steady-State Thermal Transmission Properties by Means of the Heat Flow Meter Apparatus," *Annual Book of ASTM Standards*, Vol. 4.06, American Society for Testing and Materials, West Conshohocken, PA, 2000, pp. 173, 174.

⁶Daryabeigi, K., "Heat Transfer in Adhesively Bonded Honeycomb Core Panels," AIAA Paper 2001-2825, June 2001.

⁷Stroud, C. W., "Experimental Verification of an Analytical Determination of Overall Thermal Conductivity of Honeycomb-Core Panels," NASA TN D-2866, June 1965.

⁸Fairbanks, D. R., "Effective Lateral Thermal Conductivity of Square-Cell Cores," *AIAA Journal*, Vol. 20, No. 7, 1982, pp. 1009–1014.

⁹Jones, P. D., "Combined Radiation and Conduction Heat Transfer Through Evacuated Honeycomb-Cored Panels," *Heat Transfer with Combined Modes*, American Society of Mechanical Engineers, Fairfield, NJ, HTD-Vol. 299, 1994, pp. 23–30.

¹⁰Copenhaver, D. C., Scott, E. P., and Hanuska, A., "Thermal Characterization of Honeycomb Sandwich Structures," AIAA Paper 97-2455, June 1997.

¹¹Edwards, D. K., Arnold, J. N., and Wu, P. S., "Correlations for Natural Convection Through High L/D Rectangular Cells," *Journal of Heat Transfer*, Vol. 101, No. 4, 1979, pp. 741–743.

¹²Williams, S. D., and Curry, D. M., "Thermal Protection Materials—Thermophysical Property Data," NASA RP-1289, Dec. 1992.

¹³Brown, W. F., Jr. (ed.), *Aerospace Structural Metals Handbook*, edited by C. Y. Ho, Purdue Univ. Press, West Lafayette, IN, 1994, Code 3725, p. 23.

¹⁴Kreith, F., and Black, W. Z., *Basic Heat Transfer*, Harper and Row, New York, 1980, p. 520.

¹⁵Touloukian, Y. S., Powell, R. W., Ho, C. Y., and Klemens, P. G., *Thermal Conductivity: Nonmetallic Solids*, Vol. 2, Thermophysical Properties of Matter, Plenum, New York, 1970, pp. 922–933.

¹⁶Touloukian, Y. S., and DeWitt, D. P., *Thermal Radiative Properties: Metallic Elements and Alloys*, Vol. 7, Thermophysical Properties of Matter, Plenum, New York, 1970, pp. 723–725.

¹⁷Touloukian, Y. S., and DeWitt, D. P., *Thermal Radiative Properties: Nonmetallic Solids*, Vol. 8, Thermophysical Properties of Matter, Plenum, New York, 1970, pp. 1569, 1570.

¹⁸Razelos, P., "Methods of Obtaining Approximate Solutions," *Handbook of Heat Transfer*, edited by W. M. Rohsenow and J. P. Hartnett, McGraw-Hill, New York, 1973, Chap. 4.

¹⁹Sparrow, E. M., and Cess, R. D., *Radiation Heat Transfer*, augmented ed., McGraw-Hill, New York, 1978, pp. 90–96.

²⁰Huebner, K. H., and Thornton, E. A., *The Finite Element Method for Engineers*, 2nd ed., Wiley, New York, 1982, pp. 427–430.